

Modelling and Control of a Wind Power Conversion System Based on the Double-Fed Asynchronous Generator

A.Moualdia*, MO.Mahoudi**, L.Nezli**, O.Bouchhida*

*LREA, Research Laboratory of Electronics and Automatics, University yahia fares Médéa, Algeria

**LCP, Laboratory of Process Control Dpt. Electrical Engineering, National Polytechnic School, 10, Street Pasteur, El Harrach, Algeria

†Corresponding Author; Moualdia Abdelhafidh, INSFP BP 89 Ain d'heb médéa, Algeria,+2130792150261, amoualdia1@yahoo.fr, mo.mahmoudi@enp.edu.dz, l_nezli@yahoo.fr, bouahid2000@yahoo.fr

Received: 11.03.2012 Accepted: 07.04.2012

Abstract-Wind energy has many advantages, it does not pollute and it is an inexhaustible source. However, the cost of this energy is still too high to compete with traditional fossil fuels, especially on sites less windy. The performance of a wind turbine depends on three parameters: the power of wind, the power curve of the turbine and the generator's ability to respond to wind fluctuations. This paper presents a control chain conversion based on a double-fed asynchronous machine (D.F.I.G) and flow-oriented. The supply system comprises two identical one converters connected to the rotor (RSC) and the other connected to the network (GSC) via a filter. The architecture of the device (Fig. 1) is up by three commands are necessary for the operation of the turbine control extraction of maximum power of the wind to control itself (MPPT) control of the RSC controlling the electromagnetic torque and stator reactive power and control of the GSC by controlling the DC link voltage and active power and reactive power exchanged with the network. The proposed control, has been validated in both modes of operation of the three-bladed wind 7.5kw, using the Matlab / Simulink. The results of simulation control technology study provide good dynamic performance and static.

Keywords-D.F.I.G, Variable wind speed, hypersynchronous, Energy quality, hypo synchronous

1. Introduction

The intense industrialization of recent decades and the proliferation of electrical appliances have led to global needs considerable power. Meet this demand, growing today; industrialized countries have overwhelmingly called for nuclear power plants. This energy source has the undeniable advantage of not causing air pollution unlike thermal power plants, but the risk of nuclear accident, treatment and waste disposal are very real problems that make it unattractive to the energy future generations. To address these problems, countries are turning increasingly towards the use of clean energy sources and renewable. Indeed, these countries committed themselves in the medium term, to increase their production of electricity from renewable energy.

These renewable energy sources, wind energy are one of the largest and most promising sources of renewable energy worldwide in terms of development. Especially as they are

clean and economically viable. Institutional incentives and government, together with wind energy potential and development of energy conversion technologies have enabled the rapid development of wind energy with an annual growth of 30% and a market penetration of electricity by 12% 2012 [1]. Many researches on wind turbine order were carried out. Thanks to them, the latest generation of wind turbines operate with variable speed and have a pitch regulated [2]. We can thereby change the rotational speed and the pitch angle of each blade, allowing us to improve the production of the turbine. Currently, the variable speed wind energy system based on the double-fed induction machine (D.F.I.G) is the most used in wind farms on land. Its main advantage, not least, is to have its three-phase converters designed for a portion of the nominal power of the DFIG, which makes a significant economic benefit compared to other possible solutions electromechanical conversion (machine permanent magnet synchronous for example). Indeed, the DFIG can

operate over a speed range of $\pm 30\%$ around the synchronous speed, thus ensuring a reduced sizing of static converters because they are connected between the rotor winding of the DFIG and the grid [3,4]. In the electromechanical conversion chain of wind turbine systems, static converters voltage three-phase structure are critical because they control the active and reactive power injected to the grid depending on wind speed applied on wind turbine blades. The objective of this paper is to propose a generator control that can optimize the production of the wind in both mode synchronous hyper and hypo that is to say, improve the quality of energy and energy efficiency.

The architecture of the device Fig.1 is up by three commands are necessary for the operation of the turbine control extraction of maximum power of the wind to control itself MPPT control of the RSC controlling the electromagnetic torque and stator reactive power and control of the GSC by controlling the direct current Link voltage and active power and reactive power exchanged with the network.

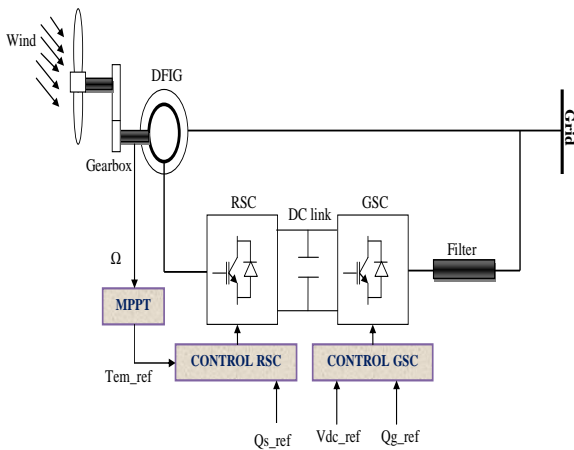


Fig.1. Architecture of the wind system.

2. Modelling of Conversion System

2.1. Modelling of the Turbine

Mechanical power available on the shaft of a wind turbine is expressed by the relation:

$$P_a = 0.5 C_p(\lambda) \pi \rho R^2 V_1^3 \tag{1}$$

The power coefficient C_p is the aerodynamic efficiency of the wind turbine. It depends on the characteristic of the turbine.

The variation of this coefficient as a function of the speed ratio λ and the orientation angle β of the blade [5].

$$C_p = f(\lambda, \beta) = c_1 \left(\frac{c_2}{\lambda_i} - C_3 - C_4 \right) \exp\left(\frac{-c_5}{\lambda_i}\right) + C_6 \lambda \tag{2}$$

With:

$$\frac{1}{\lambda_i} = \frac{1}{\lambda + 0.08\beta} - \frac{0.035}{\beta^3 + 1};$$

$C1=0.5176, C2=116, C3=0.4, C4=5, C5=21, C6=0.0068.$

The speed ratio λ is defined as the ratio between the linear speed of the blades and wind speed $\lambda = \frac{R\Omega_1}{V}$.

2.2. MPPT Bloc

The technique of extraction of the maximum power is to determine the speed of the turbine which provides the maximum generated power. The reference speed of the turbine is that corresponding to the optimum ratio of speed $\lambda_{opt} = 8.1$ (with β constant and equal to 0°) to obtain the maximum value of ($C_p = 0.47$). This control structure is to adjust the torque appearing on the turbine shaft so as to fix its speed to its reference written by $\Omega_{tur-ref} = \frac{\lambda_{opt} \cdot V}{R}$.

Especially, to extract that effectively the power of wind, while maintaining security in the system, the turbine must be operated within the three zones, which connect the wind speed, the maximum permissible rotor, and the desired power (Fig. 3). In zone I, the turbine is stopped because the wind is not strong enough for power generation is cost-effective vis-à-vis the operating energy. In zone II operation, the turbine operates at partial load. Here the objective is to maximize fuel efficiency. Thus, the rotational speed changes according to the wind speed so as to remain in the operating point of maximum aerodynamic efficiency. The goal is that the power coefficient is always optimal. Zone III, strong wind, corresponds to full load operation. We must limit the power to avoid damaging the system. To ensure maximum efficiency of the turbine, keep the power factor at its maximum [6-7]. The purpose of the proposed control strategy is to allow the couple wanted to optimize performance is beautiful and well supplied by the induction generator double-fed Tg.

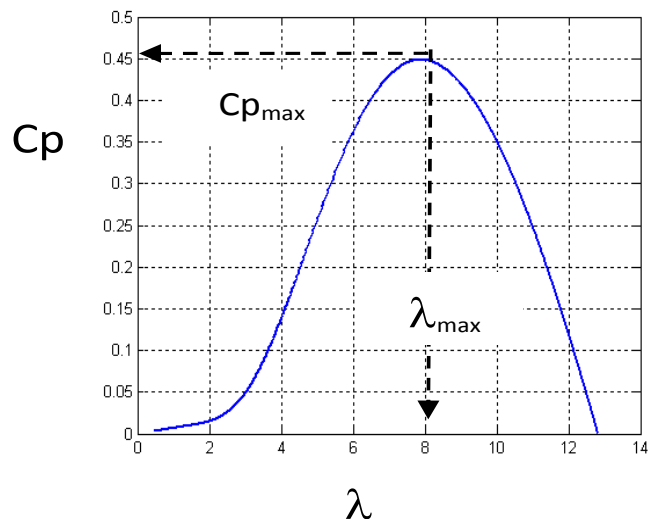


Fig.2. Power coefficient

2.3. Modelling of D.F.I.G

The generator chosen for the conversion of wind energy is a double-fed induction generator, DFIG modeling [8, 9] written in the repository of the Park, presented by the system of equations:

$$\begin{cases} V_{sd} = R_s i_{sd} + \frac{d\varphi_{sd}}{dt} - \theta_s \varphi_{sq} \\ V_{sq} = R_s i_{sq} + \frac{d\varphi_{sq}}{dt} + \theta_s \varphi_{sd} \\ V_{rd} = R_r i_{rd} + \frac{d\varphi_{rd}}{dt} - \theta_r \varphi_{rq} \\ V_{rq} = R_r i_{rq} + \frac{d\varphi_{rq}}{dt} + \theta_r \varphi_{rd} \end{cases} \quad (3)$$

$$\begin{cases} \varphi_{sd} = L_s i_{sd} + M i_{rd} \\ \varphi_{sq} = L_s i_{sq} + M i_{rq} \\ \varphi_{rd} = L_r i_{rd} + M i_{sd} \\ \varphi_{rq} = L_r i_{rq} + M i_{sq} \end{cases} \quad (4)$$

$$T_{em} = p \cdot \frac{M}{L_s} (\varphi_{sd} \cdot i_{rq} - \varphi_{sq} \cdot i_{rd}) \quad (5)$$

$$T_a = T_{em} + f \cdot \Omega + J \frac{d\Omega}{dt} \quad (6)$$

In the coordinate two-phase, the active and reactive power stator and rotor of an induction generator can be written:

$$\begin{cases} P_s = (V_{sd} i_{sd} + V_{sq} i_{sq}) \\ Q_s = (V_{sq} i_{sd} - V_{sd} i_{sq}) \end{cases} \quad (7)$$

$$\begin{cases} P_r = (V_{rd} i_{rd} + V_{rq} i_{rq}) \\ Q_r = (V_{rq} i_{rd} - V_{rd} i_{rq}) \end{cases} \quad (8)$$

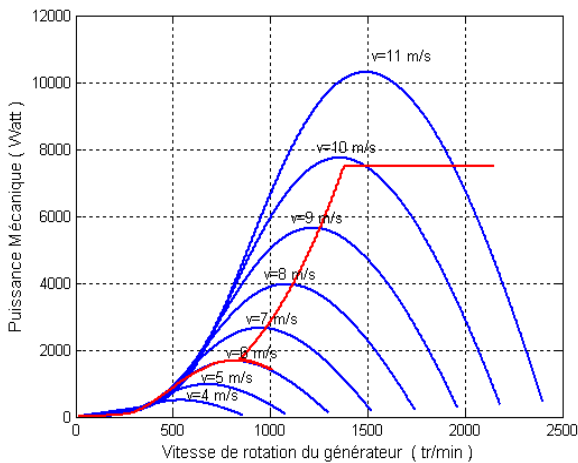


Fig.3. Typical curve of the power extracted by a wind turbine according to the wind speed

2.4. Control of Rotor Side Converter RSC

The stator flux is aligned with the axis, we assume that the network is stable and the stator flux constant set. Furthermore the generator stator resistance is negligible. [10] Since the stator flux is aligned with the axis we can write $\Psi_{sd} = \Psi_s$ and $\Psi_{sq} = 0$, equations (3), (4) and (5) become respectively:

$$V_{sd} = 0 \quad (9.a)$$

$$V_{sq} = U_s = W_s \Psi_s \quad (9.b)$$

$$\Psi_s = L_s i_{sd} + M i_{rd} \quad (9.c)$$

$$0 = L_s i_{sq} + M i_{rq} \quad (9.d)$$

$$T_{em} = p \frac{M}{L_s} \Psi_s i_{rq} \quad (9.e)$$

Or U_s is the amplitude of the stator voltage assumed constant. From equation (8.e) we can establish that the electromagnetic torque can be controlled directly by acting on the current i_{rq} , so the reference current is:

$$i_{rqref} = \frac{2L_s W_s}{3p M U_s} C_{emref} \quad (10)$$

Equation (7) of the reactive power of the stator becomes:

$$Q_s = 1.5 \frac{U_s}{L_s W_s} (U_s - M W_s i_{rd}) \quad (11)$$

From equation (10), we note that the reactive power of the stator can be controlled by varying the current i_{rd} to guarantee operation at unity power factor set point $Q_{sref} = 0$, so the reference current on the axis is:

$$i_{rdref} = \frac{U_s}{M W_s} \quad (12)$$

The control scheme of the converter on the rotor side is illustrated by Figure 4.

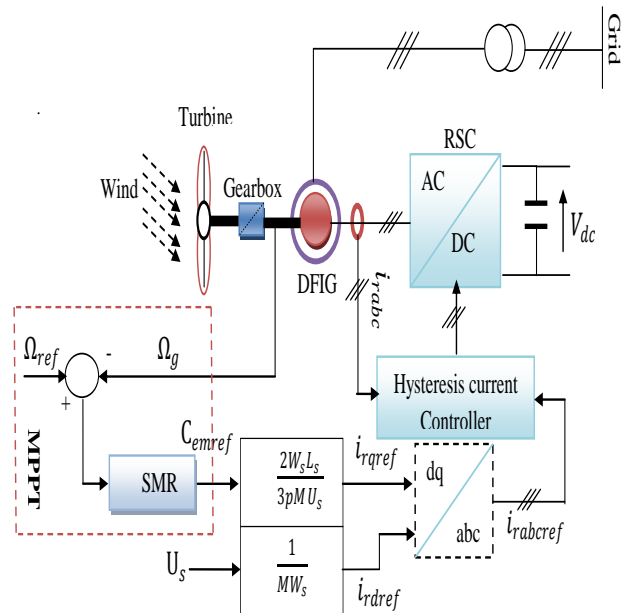


Fig.4. Control of the RSC

2.5. Grid side converter control GSC

The GSC is connected between the DC link voltage and the electrical network via an R, L filter. This converter has two roles: to maintain the DC link voltage constant regardless of the magnitude and direction of flow of the power of the DFIG rotor and maintain a unity power factor at the connection point with the grid. The command of the GSC Fig.5 performs two functions: the control currents flowing through the filter and RL control DC link. [11, 12]

The mains voltage can be expressed as follows:

$$\begin{cases} e_{ag} = R_g i_{ag} + L_g \frac{di_{ag}}{dt} + v_{ag} \\ e_{bg} = R_g i_{bg} + L_g \frac{di_{bg}}{dt} + v_{bg} \\ e_{cg} = R_g i_{cg} + L_g \frac{di_{cg}}{dt} + v_{cg} \end{cases} \quad (13)$$

Using the transformation of the park, equation (13) can be expressed as follows:

$$\begin{cases} e_{gd} = R_g i_{gd} + L_g \frac{di_{gd}}{dt} - W_s L_g i_{gq} + v_{gd} \\ e_{gq} = R_g i_{gq} + L_g \frac{di_{gq}}{dt} + W_s L_g i_{gd} + v_{gq} \end{cases} \quad (14)$$

The orientation of the voltage vector we can write:

$V_{gd} = 0$ and $V_{gq} = U_g$, with U_g is the amplitude of voltage.

Thus the expressions of active and reactive power are expressed respectively by the following equations:

$$\begin{cases} P_g = U_g i_{gq} \\ Q_g = i_{gd} U_g \end{cases} \quad (15)$$

By neglecting the losses of the converter (GSC), the continuous power must be equal to the rated active power network.

$$\begin{cases} V_{dc} i_{dc} = U_g i_{gq} \\ C \frac{dv_{dc}}{dt} = i_{dc} - i_{ond} \end{cases} \quad (16)$$

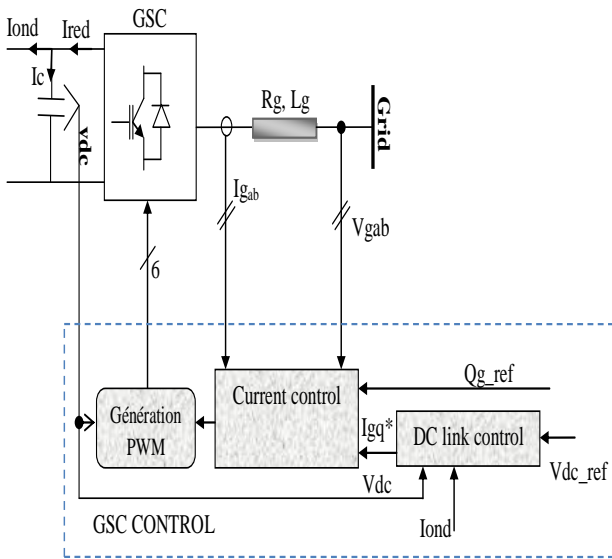


Fig.5. The principle of the converter control GSC.

2.5.1. Control currents flowing through the filter

The model of the binding of GSC network in the frame following the dq stator rotating field shows us that we can establish control of the currents flowing in the filter given RL, what about the influence of coupling, each can be controlled independently each with its own regulator. The block diagram of the control loops of the dq axes currents is written to Fig. 6 [13, 14]. The markers used are of PI type. In this scheme of regulation of compensation appear terms of dq axes. Currents and references Igd_ref and Igq_ref are

respectively from the control block of the DC link and control of reactive power at the connection point of the GSC with the grid. The direct current component is used to control the reactive power network side. The quadrature component, in turn, is used to adjust the DC link voltage. In this regulation the converter is modelled by a gain $G_c = 1$.

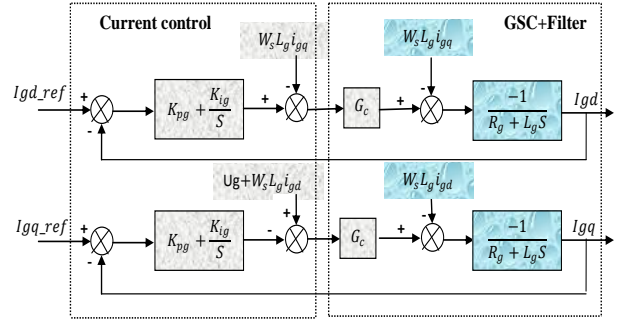


Fig.6. Control currents flowing through the filter Rg, Lg

2.6. DC Link Voltages Control.

Regulating the DC link voltage is then accomplished by an external loop (relative to the inner loop control of current), for maintaining a constant voltage on the DC link, with a PI controller generating the reference current in the capacitor. The Fig. 7 shows the block diagram of the control of the DC link voltage.

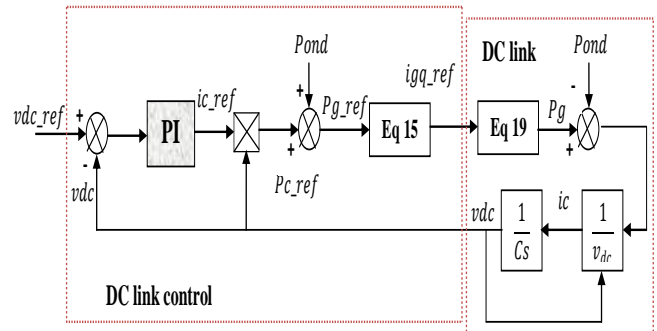


Fig.7. Control loop of the DC link voltage

The power used on the DC link can be expressed as follows:

$$\begin{aligned} P_{red} &= v_{dc} i_{red} \\ P_c &= v_{dc} i_c \end{aligned} \quad (17)$$

$$P_{ond} = v_{dc} i_{ond}$$

These powers are related by:

$$P_{red} = P_c + P_{ond} \quad (18)$$

Neglecting all losses to the Joule power exchanged between the rotor of the DFIG and the grid (losses in the capacitor, the converter and filter), we can write:

$$P_g = P_{red} = P_c + P_{ond} \quad (19)$$

The reference power for the capacitor is related to the reference current flowing in the capacitor.

$$P_{cref} = v_{dc} i_{ond}$$

In fig.7 appears P_{ond} available power corresponding to the power rotor: it's been a disturbance [14, 15] of the regulation and will be compensated in the control chain.

3. Simulation Results

Simulation results were performed using software Matlab / Simulink. To validate the controls proposed in this paper, we present two operating points in hypo-or hyper-synchronous fashion. For these simulations, we consider that the wind system is steady and working in the zone of optimal functioning (zone 2), that is to say that it produces maximum power versus speed of the wind. The reference voltage of the DC link is set at 620V. Reactive power is set at Qg_ref 0VAr, ensuring a unity power factor at the connection of the GSC with the grid. By cons, we will vary the stator reactive power Qs playing on its reference value in the control of GSC.

1) Wind power system operation mode hypo synchronous

For this mode, a wind velocity equal to 7.5m / s is applied on wind turbine blades, which corresponds to a speed of DFIG in MPPT control approximately 1044 tr/min, a shift 30% hypynchronous mode, as shown in Figure 8.

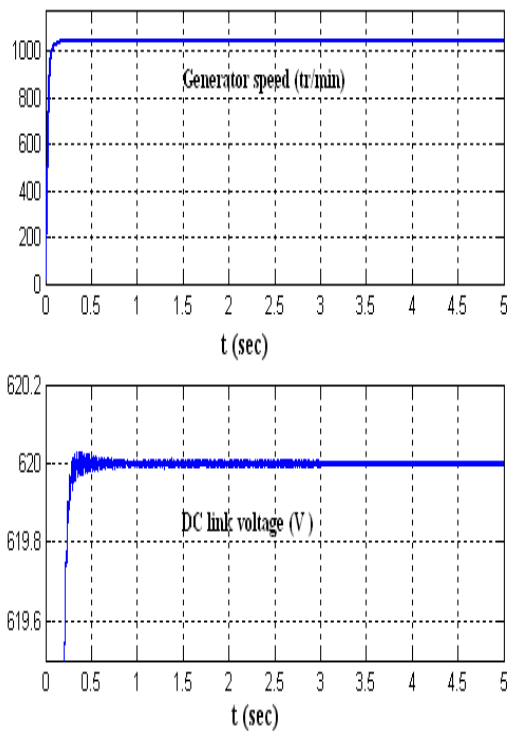


Fig. 8. Dc link voltage and generator speed (hypo synchronous)

We also observe that the DC link voltage is perfectly regulated to 620V by the GSC.

Figure 9 shows the temporal evolution of the various power supply Qs , Ps and Pr , Qr . At time $t = 1s$, the wind system operates as a unity power factor and reactive power Qs_ref Qg_ref imposed zero. From time $t = 1s$ to $t = 3s$, we set the stator reactive power reference equal to -4500Var,

corresponding to changes in the reference direct current rotor (Figure 8) and also on the rotor reactive power Qr . From time $t = 1s$ we set the stator reference reactive power equal to 4500 Var, again, different reactive powers are properly regulated.

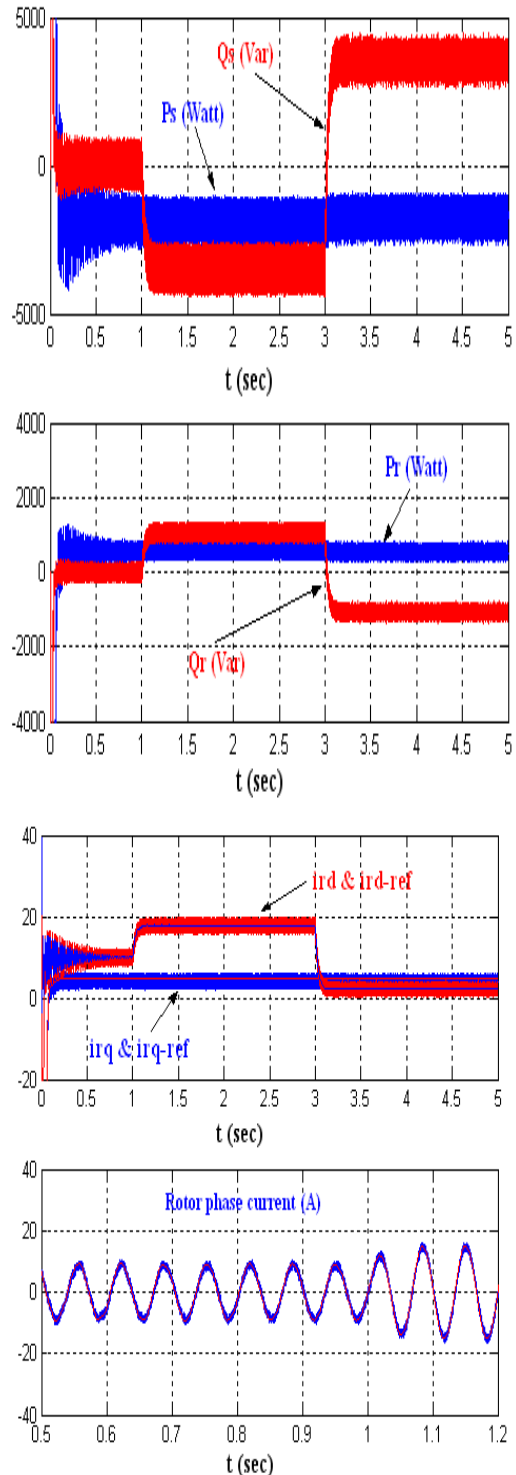


Fig. 9. Ps , Qs , Pr , Qr , ird , irq and iar (hypersynchronous)

2) Wind power system operation mode hyper synchronous

For this mode, a wind speed equal to 11.5m/s corresponds to the nominal operation of the turbine is applied

on wind turbine blades, which corresponds to a speed of DFIG in MPPT control approximately 1650 tr/min, a shift of -11% hyper synchronous mode, as shown in Figure 10 and Figure 11. The same stator reactive power variations have been applied to this mode as the previous. We also note that the dq axis rotor currents are perfectly decoupled through the decoupling strategy by ensuring natural PWM hysteresis. We also observe the rotor phase current follows perfectly the reference obtained by the orientation of the stator flux. Both modes are validated and independent control of different powers of the wind system.

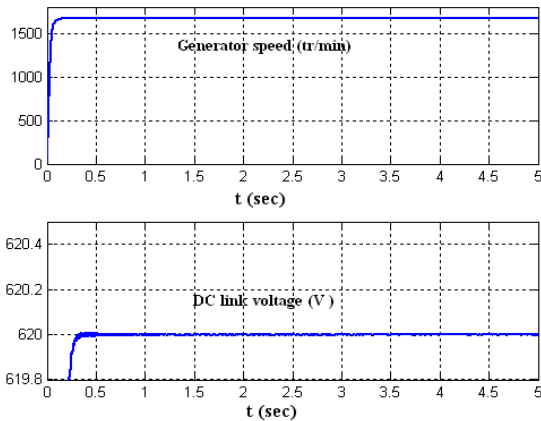


Fig. 10. Dc link voltage and generator speed (hyper synchronous)

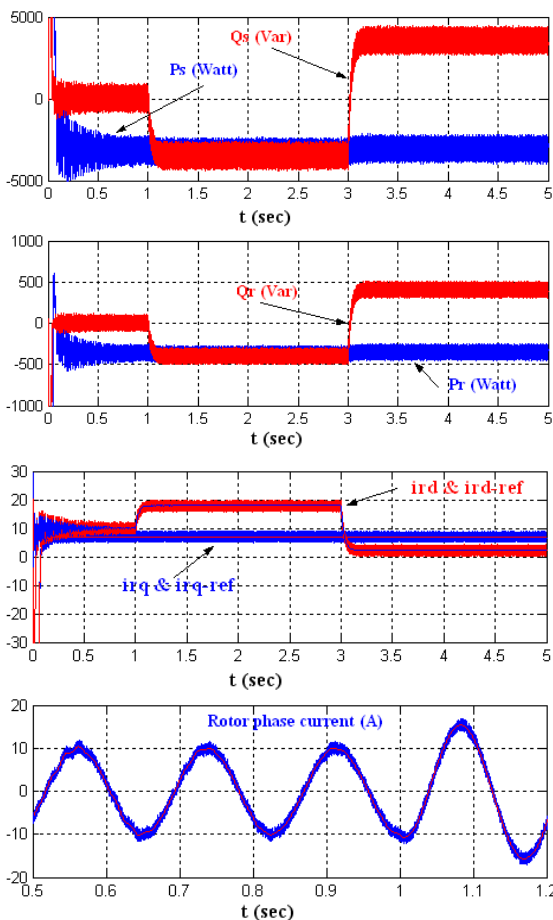


Fig. 11. Ps, Qs, Pr, Qr, ird, irq and iar (hyper synchronous)

4. Conclusion

In this paper, we presented a system for converting wind power (7.5KW) equipped with double-fed asynchronous machines. Initially, we modelled the different components of the wind system. Indeed, aerodynamic and mechanical models of the turbine. Then, in order to establish the different orders of the two converters, we have developed models of the DFIG and the binding of SAG to the network via the RL filter. In this work we have focused the study on the command in zone 2 operation allowing the wind to extract the maximum power available in the wind. The different orders of SAG and CSR were detailed to ensure independent monitoring of active and reactive power while ensuring optimum operation of the wind. Finally, to validate the proposed overall control of the wind system, we performed simulations for two operating points: one mode and the other hyposynchronous hypersynchronous mode. The results obtained showed that the active and reactive power of the wind energy system could be controlled independently while ensuring an optimal active power supplied to the grid regardless of the mode of operation.

Acknowledgements

The work presented in this publication was carried out in laboratory process control to National Polytechnic School under the scientific direction of Mr. MO. MAHMOUDI professor at the National Polytechnic School Algeria and Mr. L.Nezli teacher conference at the School National Polytechnic Algeria to whom I express my deep gratitude for all the advice and encouragement they provided during my entire duration of the different works, despite their lanky.

References

- [1] S. Peresada, A. Tilli and A. Tonielli, "Indirect Stator Flux-Oriented Output Feedback Control of a Doubly Fed Induction Machine", IEEE Transactions on Control Systems and Technology, Vol. 11, No. 6, pp. 875-888, November 2003.
- [2] Z. X. Fang, X. D. Ping and L. Y. Bing, "Predictive Functional Control of a Doubly Fed Induction Generator for Variable Speed Wind Turbines", In Proceedings of the 5th World Congress on Intelligent Control and Automation, Hangzhou, pp. 3315-3319, China, June 15-19, 2004.
- [3] G. Salloum, "Contribution à la Commande de la Machine Asynchrone à Double Alimentation", Thèse de Doctorat en Génie Electrique, Institut National Polytechnique de Toulouse, France, 2007.
- [4] Jun Yao, Hui Li, Yong Liao, and Zhe Chen, Senior Member, IEEE "An Improved Control Strategy of Limiting the DC-Link Voltage Fluctuation for a Doubly Fed Induction Wind Generator, IEEE transactions on power electronics, vol. 23, no. 3, may 2008.
- [5] R. Thresher et al., "The status and future of wind energy technology," IEEE Power & Energy Magazine, vol. 5, n°6, pp. 34-46, November/December 2007.

- [6] R. Fadaeinedjad et al., "Simulation of a wind turbine with doubly fed induction generator by FAST and Simulink," IEEE Trans. Energy Conversion, vol. 23, no. 2, pp. 690-700, June 2008.
- [7] T. Senjyu et al., "Output power levelling of wind turbine generator for all operating regions by pitch angle control," IEEE Trans. Energy Conversion, vol. 21, n°2, pp. 467-475, June 2006.
- [8] P. Poure, S. Saadate, M. Machmoum, "Variable speed DFIG wind energy system for power generation and harmonic current mitigation", Renewable Energy, Volume 34, Issue 6, June 2009, Pages 1545-1553.
- [9] A. Gaillard, "Détection de défauts des convertisseurs de puissance à l'aide de FPGA : cas d'un système éolien base sur une Machine Asynchrone à Double Alimentation (MADA)", Actes de la 8ième Conférence des Jeunes Chercheurs en Génie Electrique (JCGE'08), Ecole Centrale de Lyon, Ecully, France, pp. 202- 207, 16-17 décembre 2008.
- [10] D. Zhi and L. Xu, "Direct power control of DFIG with constant switching frequency and improved transient performance," IEEE Trans. Energy Convers., vol. 22, no. 1, pp. 110-118, Mar. 2007.
- [11] M. I. Martinez, G. Tapia, A. Susperregui, and H. Camblong, "DFIG power generation capability and feasibility regions under unbalanced grid voltage conditions," IEEE Trans. Energy Convers., vol. 26, no. 4, pp. 1051-1062, Dec. 2011.
- [12] Y. Zhou, P. Bauer, J. Ferreira, and J. Pierik, "Operation of grid-connected DFIG under unbalanced grid voltage condition," IEEE Trans. Energy Convers., vol. 24, no. 1, pp. 240-246, Mar. 2009.
- [13] J. Hu and Y. He, "Modelling and enhanced control of DFIG under unbalanced grid voltage conditions," Electr. Power Syst. Res., vol. 79, no. 2, pp. 273-281, Feb. 2009.
- [14] P.E. Vidal, Etude Commande Non-linéaire d'une Machine Asynchrone à Double Alimentation, Thèse de Doctorat, INP Toulouse 2004.
- [15] T. Senjyu et al., "Output power levelling of wind turbine generator for all operating regions by pitch angle control," IEEE Trans. Energy Conversion, vol. 21, n°2, pp. 467-475, June 2006.

Nomenclature

v	<i>wind speed (m / sec)</i>
ρ	<i>air density (kg/m³)</i>
R	<i>radius of rotor (m)</i>
P_a	<i>aerodynamic power (W)</i>
T_a	<i>Aerodynamic torque (Nm)</i>
λ	<i>specific speed</i>
$C_p(\lambda)$	<i>power coefficient</i>
$P(Q)$	<i>power (active and reactive)</i>
ϕ	<i>Flux (Wb)</i>
T_{em}	<i>electromagnetic torque (Nm)</i>
$L_s(L_r)$	<i>Stator inductance (rotor) (H)</i>
M	<i>mutual inductance (H)</i>
σ	<i>leakage coefficient $\sigma = 1 - M^2/L_sL_r$</i>
$R_s(R_r)$	<i>stator resistance (rotor) (Ω)</i>
θ_r	<i>rotor position</i>
$\omega_r(\omega_s)$	<i>Rotor and stator pulsation (rd/s)</i>
g	<i>Slip</i>
p	<i>Number of pole pairs</i>
GSC	<i>Grid side converter</i>
RSC	<i>Rotor side converter</i>
DFIG	<i>Double Fed Induction Generator</i>
MPPT	<i>Maximum point power tracking</i>